

INITIAL TSM ESTIMATION WITH HYPER-SPECTRAL IMAGES IN COASTAL WATERS BASED ON BIO-OPTIC APPROACH

Phan Minh Thu*, Bui Hong Long

Institute of Oceanography, 01 Cau Da, Nha Trang, Khanh Hoa, Vietnam

* Email: phanminhthu@vnio.org.vn

ABSTRACT

The bio-optical approaches in remote sensing applied are modelled by the relationship of remote sensing reflectance – $R_{RS}(\lambda)$ and the inherent optical properties, including backscattering - $b(\lambda)$ and absorption - $a(\lambda)$ coefficient of components in water bodies. Based on the in-situ data of bio-optics and TSM (Total Suspended Matter) concentration from surveys of Nha Trang Bay in the period of 2013-2014, the paper presents the potential application of marine bio-optics for TSM estimation from hyperspectral images in the waters. The diffuse attenuation coefficients – $K_d(\lambda)$ – and irradiance reflectance – $R_{rs}(\lambda)$ were derived from downward and upward irradiance measurement; $a(\lambda)$ was observed by UV spectrophotometer in 380 – 800nm wavelength; whereas $b(\lambda)$ was calculated from total suspended matter. The in-situ data were acquired an estimation of TSM by the ratio among $R(\lambda)$. The best relationship of model for in-situ $R_{rs}(\lambda)$ and TSM concentration would be chosen to apply for hyperspectral images. In the case of LANDSAT 8, the band ratios (bands 1 – 4) were simulated from the collected reflectance spectra and potential estimation errors were assessed. The best relationship would be applied for TSM estimation of LANDSAT 8 images. The findings indicated that the band ratio model could be applied for LANDSAT 8 (bands 1-4) or other similar hyperspectral images (like VNREDSat 1). Hyperspectral images database would be used to monitor the TSM in similar condition coastal waters similar with Nha Trang Bay.

1. INTRODUCTION

Optical reflectance of TSM (total suspended matter) in coastal water were contributed by phytoplankton, non-algal TSM and dissolved color organic matter (CDOM) (Wallace, *et al.*, 2014). The reflectance value of water components is very importance for estimation of TSM spatial distribution from remote sensing data. Several algorithms was researched to derive the concentration of TSM (Kuenzer & Tuan, 2013; Neckel & Labs, 1984; Zhang, *et al.*, 2009a; Zhang, *et al.*, 2009b). Some of them targeted using the inherent optical properties to estimate of TSM.

In Vietnam, marine optics integrated in remote sensing field of TSS concentration was presented in several publication (Phan Minh Thu, *et al.*, 2008; Tomasi, *et al.*, 1996; Yahya, *et al.*, 2014). Phan Minh Thu *et al.* (2008) mentioned that marine optical properties could be applied for estimation of TSM from LANDSAT ETM+ in Nha Trang Bay, but it had not calibrated.

This paper shows the initial results of estimating TSM concentration in Nha Trang Bay by combining bio-optic approaches within light properties for hyper-spectral images.

2. MATERIALS AND METHODS

2.1. Bio-optic modeling

Irradiance reflectance – $R(z,\lambda)$ – is defined as (Morel & Prieur, 1977):

$$R(z,\lambda) = E_u(z,\lambda) / E_d(z,\lambda)$$

where, $E_u(z,\lambda)$ and $E_d(z,\lambda)$ are upwelling and downward irradiance at depth (z) in the water column. On another hand, irradiance reflectance (R) is the function of total absorption coefficients – $a(\lambda)$ – and total backscattering coefficients – $b(\lambda)$:

$$R(0, \lambda) = f \frac{b_b(\lambda)}{a(\lambda) + b_b(\lambda)}$$

where, f is depended on the radiance distribution within the subsurface light field and on the volume scattering of particles in seawater. Kirk (2014) modeled f as function of the cosine of the solar zenith angle (μ_0) of refracted photon as $f(\mu_0) = -0.629 \mu_0 + 0.975$

The $R(\lambda,0)$ is closely related to the spectral remote sensing reflectance – $R_{rs}(\lambda)$ as (Kirk, 1994):

$$R_{rs}(\lambda, 0) = L_w(\lambda, 0)/E_d(\lambda, 0)$$

where, $L_w(\lambda,0)$ is the water leaving radiance and $E_d(\lambda,0)$ is downward irradiance above the air-water interface. According to Gordon and Morel (1983), $L_w(\lambda,0) = 0.54 L_u(\lambda,0)$ and $L_u(\lambda,0) = E_u(\lambda,0)/Q$.

Another hand, according to Ahn et al (2006), with the sensor viewing angle (10-20° from nadir), $R_{rs}(\lambda)$ can be written as follows:

$$R_{rs}(\lambda) = 0.044 \frac{b_b(\lambda)}{a(\lambda) + b_b(\lambda)}$$

Where: $b_b(\lambda) = b_{bw}(\lambda) + b_{bTSM}(\lambda)$
 $a(\lambda) = a_w(\lambda) + a_{nTSM}^*(\lambda)nTSM + a_{Chla}^*(\lambda)Chla + a_{CDOM}^*(\lambda)CDOM$
 where, a_w , a_{nTSM} , a_{Chla} , a_{CDOM} , are absorption of pure seawater, non-algal TSM and Chl-a, respectively; b_{bw} , b_{bTSM} are backscattering of pure seawater, TSM, respectively.

$$b_{bTSM}(\lambda) = b_{bTSM}^*(550) \left(\frac{550}{\lambda}\right)^y TSM$$

where, $b_{bTSM}^*(550) = 0.0086 m^2 g^{-1}$ (Kiefer & Reynolds, 1992).

2.2. Collecting samples and field measurement

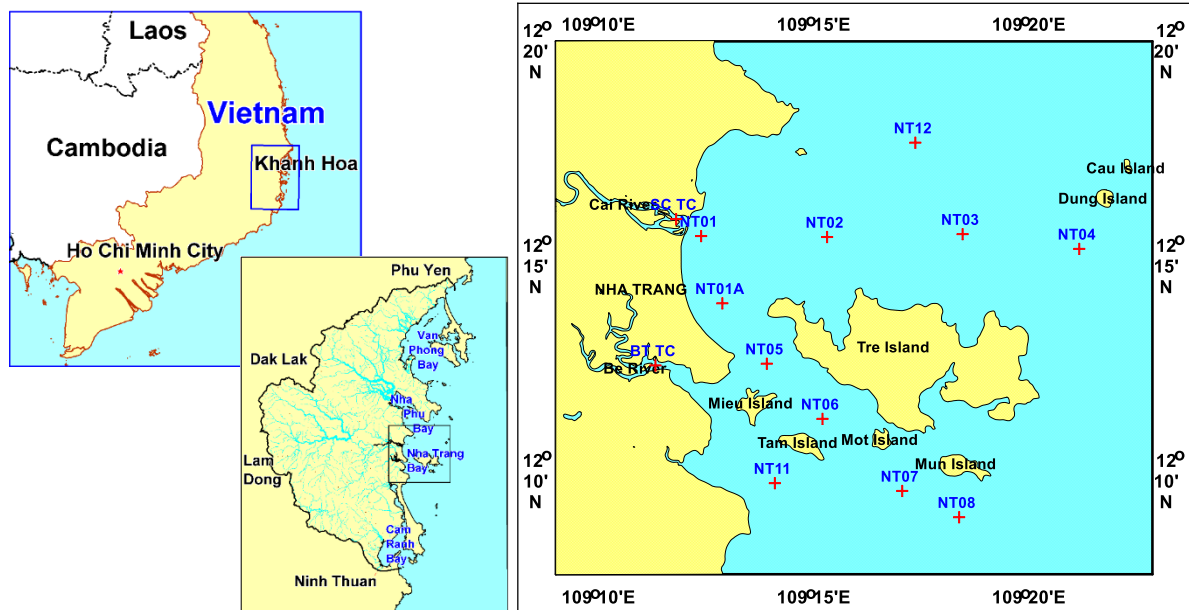


Fig. 1: Stations in Nha Trang Bay

Water samples for TSM and Chlorophyll-a (Chl-a) was collected at the 11 stations in Nha Trang Bay in the period of 2013-2014 (Fig. 1). At the same time, the light properties ($E_d(\lambda, z)$ and $L_u(\lambda, z)$) of water column at all stations also was measured by PRR2600 at light wavelength of 380, 412, 443, 490, 555, 625 and 665 nm.

2.3. Sampling measurement and estimating optics

Water samples were filtered by GF/F membranes. TSM was measured by weight method after drying at 105°C within 24 hours (APHA, 2005), whereas Chl-a was extracted by acetone 90% within 24 hours and measured by spectrophotometers (Jeffrey, *et al.*, 1997).

The attenuation coefficient for downwelling irradiance – $K_d(\lambda)$ – is computed (from 0 to a certain depth x) as:

$$K_d(\lambda) = (1/z) \ln(E_d(\lambda, 0) / E_d(\lambda, z))$$

The band characteristics of Landsat 8 and wavelength of light intensive were given in Table 1.

Table 1: Bandwidth of LANDSAT 8 and wavelength of light for calculation

| Sensor | Bands | Wavelength (micrometers) | Using PRR2600 wavelength (nm) |
|---------------------|------------------------------------|--------------------------|-------------------------------|
| LDCM – Landsat 8 | Band 1 - Coastal aerosol | 0,433 - 0,453 | 443 |
| | Band 2 – Blue | 0,450 - 0,515 | 490 |
| | Band 3 – Green | 0,525 - 0,600 | 555 |
| | Band 4 – Red | 0,630 - 0,680 | 665 |
| | Band 5 - Near Infrared (NIR) | 0,845 - 0,885 | |
| | Band 6 - SWIR 1 | 1,560 - 1,660 | |
| | Band 7 - SWIR 2 | 2,100 - 2,300 | |
| | Band 8 - Panchromatic | 0,500 - 0,680 | |
| | Band 9 - Cirrus | 1,360 - 1,390 | |
| | Band 10 - Thermal Infrared (TIR) 1 | 10,3 - 11,3 | |
| | Band 11 - Thermal Infrared (TIR) 2 | 11,5 - 12,5 | |

According to Loisel *et al.* (2014), Band blue, green and Red could be fined to estimate TSM concentration, whereas Neil *et al.* (2013) indicated that Band Red was more related with non-algal TSM.

3. RESULTS AND DISCUSSIONS

3.1. Diffuse attenuation for downward irradiance

The $K_d(\lambda)$ coefficients in Nha Trang Bay were strongly variation for the full spectrum (380 – 70nm) (Fig. 2). The $K_{d\text{PAR}}$ was significantly changed between dry season to rainy season ($p < 0.05$). They were means of $0.181 \pm 0.071 \text{ m}^{-1}$ and $0.229 \pm 0.166 \text{ m}^{-1}$, respectively. The K_d value would present the status of transparent water as well as the concentration of TSM. Less K_d would give more transparent water. The $K_{d\text{PAR}}$ for clear water was determined at 0.034 m^{-1} (Vincent, *et al.*, 1998) and $K_d(420)$ of pure water was 0.00758 m^{-1} (Morel & Maritorena, 2001). The K_d in Nha Trang Bay indicated that water bodies was case 2 water or turbidity water. In addition, Table 2 show that $K_d(\lambda)$ could be estimated from TSM.

Table 2: Relationship between TSM with total of K_d

| | TSM | TOM | TIM |
|-------|--------|--------|--------|
| TSM | 1 | | |
| TOM | 0.8231 | 1 | |
| TIM | 0.9885 | 0.7280 | 1 |
| Kd380 | 0.8109 | 0.5605 | 0.8301 |
| Kd412 | 0.8056 | 0.5478 | 0.8271 |
| Kd443 | 0.7946 | 0.5259 | 0.8195 |
| Kd490 | 0.7638 | 0.5065 | 0.7876 |
| Kd555 | 0.6936 | 0.4569 | 0.7159 |
| Kd625 | 0.6479 | 0.4154 | 0.6718 |
| Kd665 | 0.6164 | 0.3819 | 0.6426 |

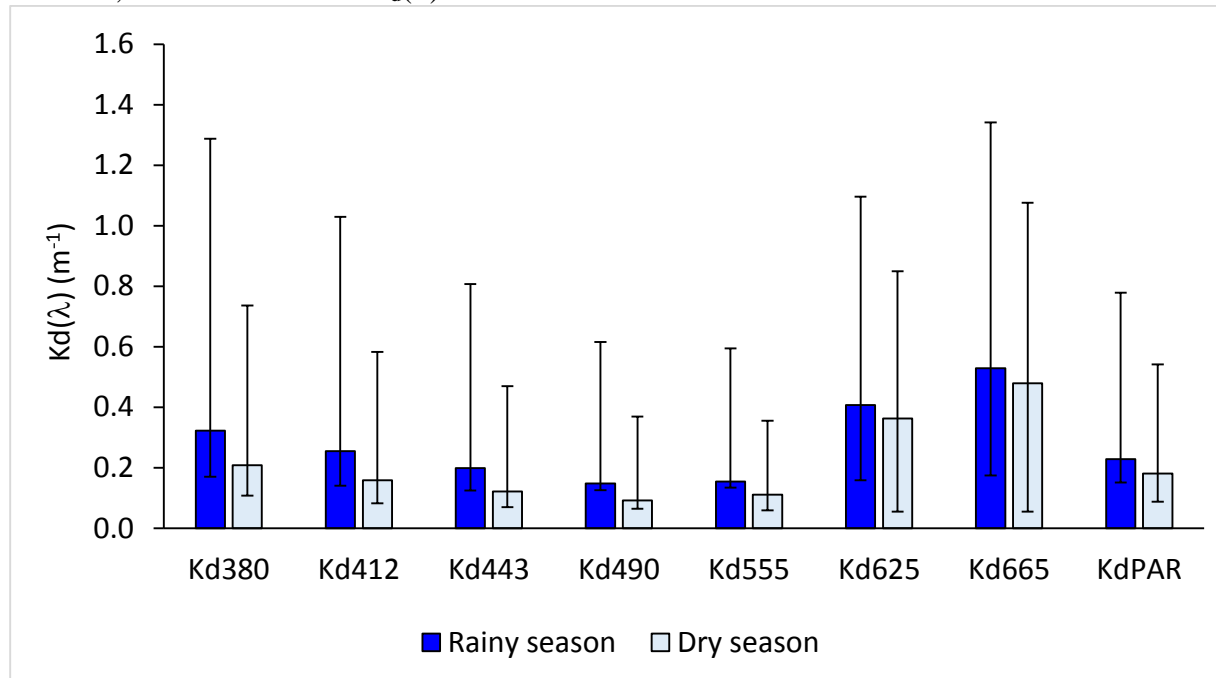


Fig. 2: Variation of $K_d(\lambda)$ average in Nha Trang Bay

3.2. TSM modeling for remote sensing estimation

Table 3: Matrix of correlation between TSM with $R_{rs}(\lambda)$

| | TSM | TOM | TIM | Rrs380 | Rrs412 | Rrs443 | Rrs490 | Rrs555 | Rrs625 |
|--------|---------------|---------|---------|--------|--------|--------|--------|--------|--------|
| Rrs380 | 0.0505 | -0.2696 | -0.1863 | 1 | | | | | |
| Rrs412 | 0.1661 | -0.1522 | -0.0827 | 0.9375 | 1 | | | | |
| Rrs443 | 0.3084 | -0.0951 | 0.0487 | 0.8886 | 0.9465 | 1 | | | |
| Rrs490 | 0.3564 | -0.0423 | 0.1398 | 0.7854 | 0.8940 | 0.9773 | 1 | | |
| Rrs555 | 0.5738 | 0.1682 | 0.4406 | 0.5653 | 0.7246 | 0.8602 | 0.9287 | 1 | |
| Rrs625 | 0.8033 | 0.2788 | 0.5937 | 0.3750 | 0.5188 | 0.6743 | 0.7352 | 0.8950 | 1 |
| Rrs665 | 0.8026 | 0.2672 | 0.5697 | 0.3783 | 0.5221 | 0.6743 | 0.7320 | 0.8882 | 0.9983 |

The related matrix between R_{rs} and TSS, TIM (Table 3 and Fig. 3) shows that reflectance value at 625 and 665nm were suitable for retrieval of TSM in coastal water. This results would be applied for red band (Band 4) of Landsat 8 or other remote sensor images with the same as band width value. Our results would be demonstrated for studies of Loisel et al. (2014) and Neil et al. (2013) for the TSM algorithms based on optic-approaches.

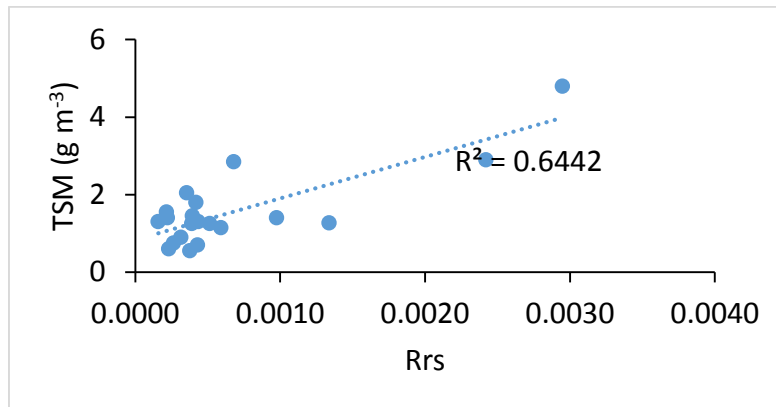


Fig. 3: TSM vs. $R_{rs}(665)$

4. CONCLUSION

By the data analysis from light intensive at 380, 412, 443, 490, 555, 625 and 665 nm; in-situ data of TSM and optical modelling, the diffuse attenuation for downward irradiance ($K_d(\lambda)$ and K_{PAR}) and reflectance (R_{rs}) were obtained in the relationship with TSM. Based on K_{PAR} , the water bodies of Nha Trang Bay was defined as case 2 water. In addition, R_{rs} at 625 and 665 nm were suitable for estimating TSM. These wavelengths were integrated in the Band 4 of Landsat 8. These results also could be applied for other remote sensing images with the similar band width at red band.

Acknowledgments

The study was supported by the project VAST.ĐLT.01/13-14 from Vietnam Academy of Science and Technology and NANO SE Asia project (2013-2014). We also would like to thank the organizers of GIS-IDEAS 2014 for their contribution.

References

- Ahn, Y.H., Shanmugam, P., Moon, J.E., 2006. Retrieval of ocean colour from high resolution multi-spectral imagery for monitoring highly dynamic ocean features. *International Journal of Remote Sensing*. 27, 367-392.
- APHA, 2005. *Standard Methods for the Examination of Water and Wastewater*, 21st Edition. American Public Health Association, Washington, D.C.,
- Jeffrey, S.W., Mantoura, R.F.C., Wright, S.W., 1997. *Phytoplankton pigments in oceanography : guidelines to modern methods*. Monographs on oceanographic methodology, UNESCO Publishing,
- Kirk, J.T.O., 1994. *Light and Photosynthesis in Aquatic Ecosystems*. Cambridge University Press,
- Kuenzer, C., Tuan, V.Q., 2013. Assessing the ecosystem services value of Can Gio Mangrove Biosphere Reserve: Combining earth-observation- and household-survey-based analyses. *Applied Geography*. 45, 167-184.

- Morel, A., Maritorena, S., 2001. Bio-optical properties of oceanic waters: A reappraisal. *Journal of Geophysical Research: Oceans*. 106, 7163-7180.
- Morel, A., Prieur, L., 1977. Analysis of Variations in Ocean Color. *Limnology and Oceanography*. 22, 709-722.
- Neckel, H., Labs, D., 1984. The solar radiation between 3300 and 12500 Å. *Solar Physics*. 90, 205-258.
- Phan Minh Thu, Schaepman, M.E., Leemans, R., Nguyen Tac An, Tong Phuoc Hoang Son, Ngo Manh Tien, Phan Thanh Bac, 2008. Water quality assessment in the Nha Trang Bay (Vietnam) by using in-situ and remotely sensed data. V. Raghavan, *et al.* (Ed.)^(Eds.). International Symposium on GIS-IDEAS 2010, Ha Noi, Vietnam, 4-6 Dec 2008, JVGC Technical Document No.4, 253-258.
- Tomasi, C., Di Giuseppe, F., Cappelli, L., Vitale, V., 1996. Average spectral curves of extraterrestrial solar irradiance in the (180–400) nm wavelength range. *Il Nuovo Cimento C*. 19, 591-618.
- Vincent, W.F., Rae, R., Laurion, I., Howard-Williams, C., Priscu, J.C., 1998. Transparency of Antarctic ice-covered lakes to solar UV radiation. *Limnology and Oceanography*. 43, 618-624.
- Wallace, R.B., Baumann, H., Grear, J.S., Aller, R.C., Gobler, C.J., 2014. Coastal ocean acidification: The other eutrophication problem. *Estuarine, Coastal and Shelf Science*. 148, 1-13.
- Yahya, N.N., Hashim, M., Ahmad, S., 2014. Remote Sensing of shallow sea floor for digital earth environment. *IOP Conference Series: Earth and Environmental Science*. 18, 012110.
- Zhang, X., Hu, L., He, M.-X., 2009a. Scattering by pure seawater: Effect of salinity. *Optics Express*. 17, 5698-5710.
- Zhang, Y., Liu, M., van Dijk, M.A., Zhu, G., Gong, Z., Li, Y., Qin, B., 2009b. Measured and numerically partitioned phytoplankton spectral absorption coefficients in inland waters. *Journal of Plankton Research*. 31, 311-323.